Contribution from the Departments of Chemistry, Sinsheimer Laboratories, University of California, Santa Cruz, California 95064, and University of California, Davis, California 95616

Pentacoordinated Nickel(II) Complexes with Thiolato Ligation: Synthetic Strategy, Structures, and Properties

Narayan Baidya, Marilyn Olmstead,† and Pradip K. Mascharak*

Received August 29, 1990

Reaction of $[Ni(terpy)Cl_2]$ with 2 equiv of thiolates in methanol or acetonitrile affords, depending on the basicity and bulk of the thiolate, the thiolato-bridged dimer $[Ni(terpy)(SPh)_2]_2\cdot 6CH_3OH$ (**1**), solvated monomer $[Ni(terpy)(SC_6F_5)_2(CH_3CN)]\cdot 3CH_3CN$ (**2**) and the desired pentacoordinated $[Ni(terpy)(S\text{-}2,4,6\text{-}(i\text{-}Pr)_3C_6H_2)_2]\cdot 1.5CH_3CN$ (**3**). Complex **1** crystallizes in the monoclinic space group $P2_1/c$, with $a = 9.908$ (2) Å, $b = 20.441$ (6) Å, $c = 14.340$ (4) Å, $\beta = 102.20$ (2)°, $V = 2839$ (1) Å, and $Z = 2$. The structure of **1** was refined to $R = 5.2\%$ on the basis of 2590 ($I > 3\sigma(I)$) data. Complex **2** also crystallizes in the monoclinic space group $P2_1/c$, with $a = 10.197$ (3) Å, $b = 31.659$ (7) Å, $c = 11.431$ (3) Å, $\beta = 105.58$ (2)°, $V = 3554.6$ (6) Å^3, and $Z = 4$. On the basis of 2618 ($I > 4\sigma(I)$) data, the structure was refined to $R = 7.85\%$. Complex **3** crystallizes in the triclinic space group $P\bar{1}$ with $a = 16.786$ (6) Å, $b = 17.266$ (6) Å, $c = 18.534$ (7) Å, $\alpha = 68.34$ (3)°, $\beta = 64.57$ (3)°, $\gamma = 71.93$ (3)°, $V = 4286$ (3) Å^3, and $Z = 4$. The structure of **3** was refined to 8.06% by using 8587 ($I > 4\sigma(I)$) data. In **1** and **2**, the coordination geometry around nickel is distorted octahedral while that in **3** is distorted trigonal bipyramidal. In donor solvents, **1** splits into two solvated monomers. The NMR peaks corresponding to the protons of the thiolate ligands in **1**–**3** have been assigned. In DMF, complexes **2** and **3** are reduced by $Na_2S_2O_4$ to generate $[Ni(terpy)(SR)_2]^-$, R = C_6F_5, 2,4,6-$(i\text{-}Pr)_3C_6H_2$ (**4**), which are rather unstable. Binding of CO to **4** affords $[Ni(terpy)(SR)_2(CO)]^-$, R = C_6F_5, 2,4,6-$(i\text{-}Pr)_3C_6H_2$ (**5**). These CO adducts are quite stable at low temperatures. The EPR spectra of **4** and **5** have been discussed. Evidence for binding of H^- to the nickel center in $[Ni(terpy)(S\text{-}2,4,6\text{-}(i\text{-}Pr)_3C_6H_2)_2]$ is also presented.

Introduction

Recent spectroscopic studies indicate that the nickel-containing active site (Ni site) of several Fe–Ni hydrogenases consists of a five- or six-coordinated nickel center with two to three S donors in the first coordination sphere.[1-5] The remaining donors are presumably O and/or N atoms derived from amino acids of the peptide framework. The low redox potential of the nickel site further suggests that the S donors are most probably negative polarizable sulfurs such as thiolates.[6] Since the spectral studies rely heavily on model compounds, there is an urgent need for suitable nickel complexes with $(N/O)_xS_{5-x}$ and $(N/O)_xS_{6-x}$ (where S is thiolato sulfur) chromophores. Unfortunately, very few nickel(II) complexes with $(N/O)_xS_{6-x}$ chromophore have been structurally characterized,[7,8] and to date, no pentacoordinated nickel complex with the $(N/O)_xS_{5-x}$ chromophore has been reported. As part of our systematic synthetic analogue approach to the Ni site of Fe–Ni hydrogenases, we have been involved in syntheses of nickel complexes of different coordination geometries with varying number of thiolate ligands.[8-11] So far, the reported geometries include tetrahedral,[9] square-planar,[10,11] and distorted octahedral.[8] In this paper, we report results of our attempts toward the synthesis of a five-coordinated nickel(II) complex with the N_3S_2 chromophore. Depending on the inherent basicity and the steric requirements of the thiolate ligand, the present synthetic strategy has led to bridged-octahedral (I), solvated-octahedral (II), and the desired five-coordinated (III) species. Data on binding of CO and H^- at the sixth site of nickel in the reduced forms of the type II and type III complexes are also included.

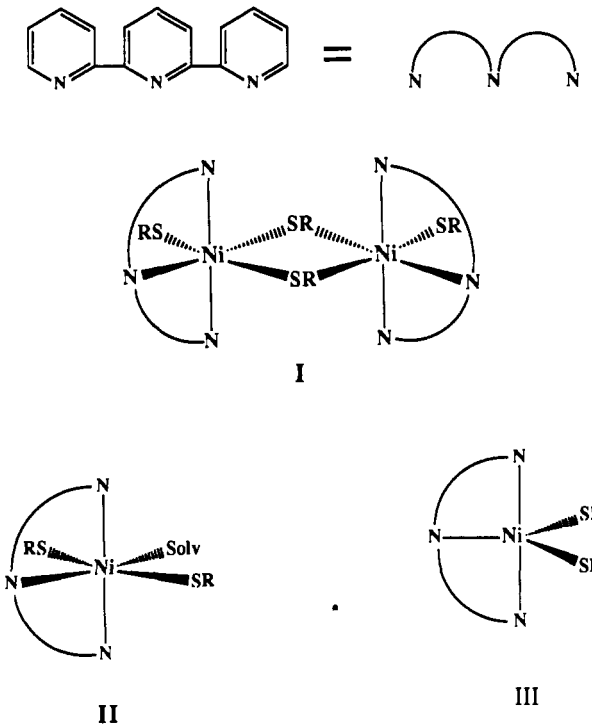

Experimental Section

Preparation of Compounds. 2,2′:6′,2″-Tripyridine (terpy), thiophenol, and pentafluorothiophenol were purchased from Aldrich Chemical Co. and were used without further purification. $[Ni(terpy)Cl_2]$ and 2,4,6-triisopropylthiophenol (TIPTP) were synthesized by following the published procedures.[12,13] In the following preparations, degassed solvents were used and all manipulations were performed under an atmosphere of pure and dry dinitrogen.

$[Ni(terpy)(SPh)_2]_2\cdot 6CH_3OH$ (1). A solution of 325 mg (1.36 mmol) of Et_4NSPh[9] in 25 mL of methanol was slowly added with stirring to a solution of 225 mg (0.62 mmol) of $[Ni(terpy)Cl_2]$ in 25 mL of methanol, causing the color of the mixture to turn dark brown. The dark brown microcrystalline precipitate, which started forming within a few minutes, was collected by filtration after 2 h of stirring at room temperature. The filtrate was stored at 4 °C for 12 h whereupon dark blocks, suitable for X-ray studies, were deposited. Combined yield: 165 mg (42%). Anal.

* To whom correspondence should be addressed at the University of California, Santa Cruz.
† University of California, Davis.

(1) Eidsness, M. K.; Sullivan, R. J.; Scott, R. A. In *The Bioinorganic Chemistry of Nickel*; Lancaster, J. R., Ed.; VCH Publishers: New York, 1988; Chapter 4.
(2) Hausinger, R. P. *Microbiol. Rev.* **1987**, *51*, 22.
(3) (a) Maroney, M. J.; Colpas, G. J.; Bagyinka, C. *J. Am. Chem. Soc.* **1990**, *112*, 7067. (b) Colpas, G. J.; Maroney, M. J.; Bagyinka, C.; Kumar, M.; Willis, W.; Mascharak, P. K. *Inorg. Chem.*, in press.
(4) X-ray absorption spectra obtained on hydrogenases from some chemotrophs have been interpreted in terms of largely S donor environments.[5]
(5) (a) Lindahl, P. A.; Kojima, N.; Hausinger, R. P.; Fox, J. A.; Teo, B. K.; Walsh, C. T.; Orme-Johnson, W. H. *J. Am. Chem. Soc.* **1984**, *106*, 3062. (b) Scott, R. A.; Wallin, S. A.; Czechowski, M.; Der Vartanian, D. V.; LeGall, J.; Peck, H. D., Jr.; Moura, I. *J. Am. Chem. Soc.* **1984**, *106*, 6864.
(6) Krüger, H. J.; Holm, R. H. *J. Am. Chem. Soc.* **1990**, *112*, 2955.
(7) Osakada, K.; Yamamoto, T.; Yamamoto, A.; Takenaka, A.; Sasada, Y. *Acta Crystallogr., Sect. C: Cryst. Struct. Commun.* **1984**, *C40*, 85.
(8) Rosenfield, S. G.; Berends, H. P.; Gelmini, L.; Stephan, D. W.; Mascharak, P. K. *Inorg. Chem.* **1987**, *26*, 2792.

0020-1669/91/1330-0929$02.50/0

Table I. Summary of Crystal Data, Intensity Collection, and Structure Refinement Parameters for $[Ni(terpy)(SPh)_2]_2 \cdot 6CH_3OH$ (**1**), $[Ni(terpy)(C_6F_5S)_2(CH_3CN)] \cdot 3CH_3CN$ (**2**), and $[Ni(terpy)(S\text{-}2,4,6\text{-}(i\text{-}Pr)_3C_6H_2)_2] \cdot 1.5CH_3CN$ (**3**)

	1	**2**	**3**
formula	$C_{60}H_{66}N_6S_4O_6Ni_2$	$C_{35}H_{23}N_7F_{10}S_2Ni$	$C_{48}H_{59.5}N_{4.5}S_2Ni$
mol wt	1212.88	854.40	822.31
color and habit	red plates	red plates	red plates
cryst syst	monoclinic	monoclinic	triclinic
space group	$P2_1/c$	$P2_1/c$	$P\bar{1}$
a, Å	9.908 (2)	10.197 (3)	16.786 (6)
b, Å	20.441 (6)	31.659 (7)	17.266 (6)
c, Å	14.340 (4)	11.431 (3)	18.534 (7)
β, deg	102.20 (2)	105.58 (2)	64.57 (3) [α = 68.34 (3)°, γ = 71.93 (3)°]
V, Å^3	2839 (1)	3554.6 (6)	4286 (3)
Z	2	4	4
cryst dimens, mm	0.25 × 0.40 × 0.40	0.14 × 0.23 × 0.90	0.20 × 0.44 × 0.52
d_{calcd}(130 K), g cm^3	1.42	1.597	1.232
μ(Mo Kα), cm^{-1}	8.62	7.48	5.65
transm coeff	0.71–0.83	0.86–0.97	0.89–0.91
scan method	ω, 2.2° range, 1.5° offset for bkgnd	ω, 1.7° range, 1.0° offset for bkgnd	ω, 0.9° range, 0.9° offset for bkgnd
2θ range, deg	0–45	0–45	0–50
no. of data collcd	4100	5139	15533
no. of unique data	3719	4634	15533
no. of data used in refinement	2590 [$I > 3\sigma(I)$]	2618 [$I > 4\sigma(I)$]	8587 [$I > 4\sigma(I)$]
no. of param refined	368	248	479
R^a	0.052	0.0785	0.0806
$R_w{}^b$	0.048 [$w^{-1} = \sigma^2(F_o)$]	0.066 [$w^{-1} = \sigma^2(F) + 0.0001F^2$]	0.086 [$w^{-1} = \sigma^2(F) + 0.0007F^2$]
GOF	1.25	1.82	1.32

$^a R = \sum||F_o| - |F_c||/|F_o|$. $^b R_w = \sum||F_o - F_c||w^{1/2}/\sum|F_o w^{1/2}|$.

Calcd for $C_{60}H_{66}N_6S_4O_6Ni_2$: C, 59.40; H, 5.49; N, 6.93. Found: C, 59.21; H, 5.53; N, 6.81. Selected IR bands (KBr pellet, cm^{-1}): 3050 (w), 1572 (s), 1447 (s), 1155 (m), 1079 (s), 766 (s), 730 (s), 695 (s), 485 (m). Value of μ_{eff} (298 K, polycrystalline): 2.98 μ_B/Ni atom.

[Ni(terpy)(SC$_6$F$_5$)$_2$(CH$_3$CN)]·3CH$_3$CN (2). A solution of $Me_4NSC_6F_5$ was prepared from 150 mg (0.75 mmol) of C_6F_5SH and 136 mg (0.75 mmol) of $Me_4NOH \cdot 5H_2O$ in 10 mL of methanol. This solution was slowly added to a solution of 123 mg (0.34 mmol) of $[Ni(terpy)Cl_2]$ in 15 mL of methanol. The color of the reaction mixture turned reddish brown, and a brown microcrystalline precipitate appeared within a minute. The reaction mixture was stirred for 5 h, and the compound was collected by filtration. Following drying in vacuo (183 mg, 52%), the compound was dissolved in warm acetonitrile and then slowly cooled to 5 °C. Dark blocks, suitable for X-ray work, were obtained in 30% yield. Anal. Calcd for $C_{35}H_{23}N_7F_{10}S_2Ni$: C, 49.16; H, 2.71; N, 11.48. Found: C, 49.02; H, 2.65; N, 11.27. Selected IR bands (KBr pellet, cm^{-1}): 3055 (w), 1600 (m), 1506 (m), 1472 (s), 1080 (s), 1014 (m), 970 (s), 856 (s), 772 (s). Value of μ_{eff} (298 K, polycrystalline): 3.18 μ_B.

[Ni(terpy)(S-2,4,6-(*i*-Pr)$_3$C$_6$H$_2$)$_2$]·1.5CH$_3$CN (3). A solution of $Me_4N(S\text{-}2,4,6\text{-}(i\text{-}Pr)_3C_6H_2)$, prepared from 162 mg (0.89 mmol) of $Me_4NOH \cdot 5H_2O$ and 211 mg (0.89 mmol) of TIPTP in 20 mL of acetonitrile was added to a suspension of 150 mg (0.41 mmol) of $[Ni(terpy)Cl_2]$ in 20 mL of acetonitrile. The color of the mixture turned brown, and as stirring continued, the light green crystals of $[Ni(terpy)Cl_2]$ disappeared while the desired product appeared as dark brown microcrystals. The reaction mixture was stirred for 5 h, and the compound was collected by filtration and dried under partial vacuum (250 mg, 74%). Recrystallization from warm acetonitrile afforded crystals for diffraction studies. Anal. Calcd for $C_{48}H_{59.5}N_{4.5}S_2Ni$: C, 70.04; H, 7.29; N, 7.66. Found: C, 70.12; H, 7.18; N, 7.51. Value of μ_{eff} (298 K, polycrystalline): 3.23 μ_B.

The complex $[Ni(terpy)(S\text{-}C_6H_4\text{-}p\text{-}CH_3)_2]_2$ was synthesized in 65% yield by following this procedure and was characterized by spectroscopic studies (vide infra).

The synthesis of $[Ni(terpy)(SPh)_2]_2$ has also been repeated in acetonitrile. The yield was higher (84%) though better crystals were obtained from methanol (procedure mentioned above).

X-ray Data Collection, Structure Solution, and Refinement. Diffraction experiments were performed at 130 K either on a Syntex $P2_1$ or a Siemens R3m/V machine, both equipped with a graphite monochromator and a modified LT-1 low-temperature apparatus. Mo Kα radiation (λ = 0.71069 Å) was employed. Only random fluctuations of less than 2% in the intensities of three standard reflections were observed during the course of data collection. The structures of **1** and **3** were solved by Patterson and difference Fourier methods while that of **2** was solved by direct methods.[14,15] Hydrogen atoms bonded to the carbon atoms were included at calculated positions by using a riding model, with C–H of 0.96 Å and $U_H = 1.2U_C$. The data were corrected for absorption effects by use of the program XABS.[16]

The asymmetric unit of **1** contains three molecules of methanol in addition to half of the dimeric complex. Two of the methanol molecules are ordered and participate in hydrogen bonding. The third one is disordered and was modeled with two positions for the oxygen atom with refined occupancies of 58 (4) and 42 (4)% for O(3a) and O(3b), respectively. The two ordered hydroxyl hydrogens were located on a final difference map and refined with the constraints O–H = 0.85 Å, U = 0.06 Å^2, and tetrahedral C–O–H angle. In the final cycles of refinement, non-hydrogen atoms were assigned anisotropic thermal parameters. The largest feature on a final difference map was 0.04 e Å^{-3} in height.

As is the case with **1**, the space group determination for **2** was unambiguous. The structure was refined by full-matrix least-squares methods. Anisotropic thermal parameters were assigned to Ni and S atoms in the final cycles of refinement. The space group of **3** was either $P\bar{1}$ or $P1$; successful solution and refinement were obtained in the former. Final refinement was carried out with anisotropic thermal parameters for Ni and S atoms only. The two molecules in the asymmetric unit (vide infra) were refined in blocks. Methyl hydrogens were located in difference maps and subsequently refined as rigid groups. The largest features on

(9) Rosenfield, S. G.; Armstrong, W. H.; Mascharak, P. K. *Inorg. Chem.* **1986**, *25*, 3014.
(10) Rosenfield, S. G.; Wong, M. L. Y.; Stephan, D. W.; Mascharak, P. K. *Inorg. Chem.* **1987**, *26*, 4119.
(11) (a) Baidya, N.; Olmstead, M. M.; Mascharak, P. K. *Inorg. Chem.* **1989**, *28*, 3426. (b) Baidya, N.; Stephan, D. W.; Campagna, C. F.; Mascharak, P. K. *Inorg. Chim. Acta* **1990**, *177*, 233. (c) Baidya, N.; Olmstead, M. M.; Mascharak, P. K. *Inorg. Chem.*, submitted for publication.
(12) Judge, J. S.; Reiff, W. M.; Intille, G. M.; Ballway, P.; Baker, W. A. *J. Inorg. Nucl. Chem.* **1967**, *29*, 1711.
(13) Blower, P. J.; Dilworth, J. R.; Hutchinson, J.; Zubieta, J. A. *J. Chem. Soc., Dalton Trans.* **1985**, 1533.
(14) SHELXTL, version 5.1, installed on a Data General Eclipse computer; SHELXTL PLUS, installed on a MicroVAX 3200 computer.
(15) Neutral-atom scattering factors and corrections for anomalous dispersion were taken from: *International Tables for X-ray Crystallography*; Kynoch Press: Birmingham, England, 1974; Vol. IV.
(16) Moezzi, B. Ph.D. Dissertation, University of California, Davis, 1987. The program obtains an absorption tensor from F_o - F_c differences.

Table II. Atomic Coordinates ($\times 10^4$) and Isotropic Thermal Parameters ($Å^2 \times 10^3$) for $[Ni(terpy)(SPh)_2]_2 \cdot 6CH_3OH$ (**1**)[a]

	x	y	z	U
Ni	3646 (1)	684 (1)	4519 (1)	19 (1)*
S(1)	3497 (2)	1398 (1)	3148 (1)	26 (1)*
S(2)	5779 (2)	221 (1)	4270 (1)	20 (1)*
N(1)	2051 (5)	104 (2)	3723 (3)	24 (2)*
N(2)	1972 (5)	1024 (2)	4930 (3)	22 (2)*
N(3)	4462 (5)	1435 (2)	5459 (3)	22 (2)*
O(1)	7647 (5)	676 (3)	−582 (4)	61 (2)*
Ho(1)	7736	386	−990	60
O(2)	2489 (5)	599 (2)	1202 (3)	51 (2)*
Ho(2)	3146	622	1689	60
C(1)	2173 (6)	−359 (3)	3096 (4)	26 (2)*
C(2)	1056 (6)	−684 (3)	2558 (4)	34 (2)*
C(3)	−228 (7)	−528 (3)	2670 (5)	41 (3)*
C(4)	−391 (7)	−53 (3)	3313 (5)	38 (3)*
C(5)	778 (6)	264 (3)	3841 (4)	25 (2)*
C(6)	720 (6)	786 (3)	4517 (4)	29 (2)*
C(7)	−473 (7)	1052 (3)	4739 (5)	37 (3)*
C(8)	−337 (7)	1563 (3)	5372 (5)	41 (3)*
C(9)	944 (6)	1808 (3)	5801 (5)	33 (2)*
C(10)	2099 (6)	1529 (3)	5541 (4)	27 (2)*
C(11)	3535 (6)	1757 (3)	5859 (4)	25 (2)*
C(12)	3934 (7)	2267 (3)	6480 (4)	35 (3)*
C(13)	5275 (7)	2461 (4)	6721 (5)	46 (3)*
C(14)	6233 (7)	2129 (4)	6311 (5)	49 (3)*
C(15)	5778 (7)	1625 (3)	5685 (5)	35 (2)*
C(16)	1962 (6)	1836 (3)	3069 (4)	27 (2)*
C(17)	711 (6)	1620 (3)	2517 (5)	34 (2)*
C(18)	−501 (7)	1949 (3)	2502 (5)	39 (3)*
C(19)	−520 (7)	2522 (4)	3024 (5)	46 (3)*
C(20)	707 (7)	2762 (3)	3545 (5)	42 (3)*
C(21)	1938 (7)	2425 (3)	3570 (4)	34 (2)*
C(22)	5931 (5)	172 (3)	3064 (4)	20 (2)*
C(23)	5696 (6)	−415 (3)	2548 (4)	28 (2)*
C(24)	5830 (6)	−447 (3)	1600 (4)	35 (2)*
C(25)	6185 (7)	99 (3)	1161 (4)	37 (3)*
C(26)	6416 (6)	682 (3)	1657 (4)	34 (2)*
C(27)	6295 (5)	719 (3)	2604 (4)	24 (2)*
C(28)	8950 (8)	760 (4)	39 (6)	68 (4)*
C(29)	2710 (8)	1098 (4)	559 (5)	54 (3)*
C(30)	6267 (12)	2104 (4)	9211 (7)	95 (5)*
O(3A)	6602 (9)	1691 (4)	8503 (7)	62 (4)*
O(3B)	6380 (15)	2793 (9)	8988 (10)	93 (7)*

[a] An asterisk denotes the equivalent isotropic U defined as one-third of the trace of the orthogonalized U_{ij} tensor.

final difference maps were 0.75 and 0.85 e $Å^{-3}$ in height for **2** and **3** respectively.

Machine parameters, crystal data, and data collection parameters are summarized in Table I. The following data are tabulated: positional parameters (Tables II–IV) and selected bond distances and angles (Table V). The rest of the crystallographic data has been submitted as supplementary material.

Other Physical Measurements. Infrared spectra were obtained with a Perkin-Elmer 1600 FTIR spectrometer. Absorption spectra were recorded on a Perkin-Elmer Lambda 9 spectrophotometer. ^1H NMR spectra were measured on a General Electric 300-MHz GN-300 instrument. Samples were dissolved in $(CD_3)_2SO$ (99.5% D). A Johnson Matthey magnetic susceptibility balance was used to monitor the room-temperature susceptibility values in the polycrystalline state. Diamagnetic corrections were calculated from the Pascal constants.[17] EPR spectra were obtained at X-band frequencies by using a Bruker ESP-300 spectrometer. Elemental analyses were performed by Atlantic Microlabs Inc., Atlanta, GA.

Results and Discussion

Syntheses of mononuclear mixed-ligand complexes are often beset with problems arising from disproportionation and other equilibria. When thiolate ligands are involved, such attempts face additional difficulties due to formation of multinuclear species including insoluble polymers. In order to avoid these problems

(17) Mulay, L. N. In *Physical Methods of Chemistry*; Weissberger, A., Rossiter, B. W., Eds.; Wiley-Interscience: New York, 1972; Part IV, Chapter VII.

Table III. Atomic Coordinates ($\times 10^4$) and Equivalent Isotropic Displacement Coefficients ($Å^2 \times 10^3$) for $[Ni(terpy)(SC_6F_5)_2(NCCH_3)] \cdot 3CH_3CN$ (**2**)

	x	y	z	U(eq)[a]
Ni	2648 (2)	1596 (1)	−215 (1)	20 (1)
S(1)	4584 (3)	1556 (1)	−1141 (2)	24 (1)
C(11)	5980 (11)	1486 (3)	117 (9)	23 (3)
C(12)	6694 (10)	1815 (3)	783 (9)	20 (3)
C(13)	7744 (11)	1773 (3)	1815 (10)	27 (3)
C(14)	8144 (11)	1371 (3)	2232 (9)	24 (3)
C(15)	7524 (11)	1029 (3)	1597 (9)	26 (3)
C(16)	6462 (11)	1085 (3)	590 (10)	26 (3)
F(12)	6328 (6)	2218 (2)	426 (5)	33 (2)
F(13)	8368 (6)	2104 (2)	2442 (5)	37 (2)
F(14)	9205 (6)	1321 (2)	3239 (5)	37 (2)
F(15)	7929 (6)	633 (2)	1997 (6)	40 (2)
F(16)	5840 (6)	733 (2)	−3 (5)	34 (2)
S(2)	682 (3)	1570 (1)	699 (2)	24 (1)
C(21)	−697 (10)	1457 (3)	−557 (9)	15 (3)
C(22)	−1127 (11)	1046 (3)	−907 (9)	25 (3)
C(23)	−2176 (11)	962 (3)	−1912 (10)	29 (3)
C(24)	−2856 (11)	1279 (4)	−2596 (10)	33 (3)
C(25)	−2508 (10)	1687 (3)	−2283 (9)	25 (3)
C(26)	−1455 (11)	1768 (3)	−1272 (10)	30 (3)
F(22)	−504 (6)	711 (2)	−235 (5)	35 (2)
F(23)	−2549 (6)	548 (2)	−2202 (6)	44 (2)
F(24)	−3879 (6)	1191 (2)	−3614 (5)	41 (2)
F(25)	−3180 (6)	2007 (2)	−2975 (6)	41 (2)
F(26)	−1159 (6)	2181 (2)	−980 (5)	32 (2)
N(1)	2601 (10)	950 (3)	−229 (8)	28 (2)
C(2)	2545 (12)	599 (3)	−226 (10)	27 (3)
C(3)	2455 (14)	140 (3)	−223 (12)	52 (4)
N(3)	1448 (8)	1728 (3)	−1962 (7)	20 (2)
C(31)	865 (10)	1458 (3)	−2817 (9)	23 (3)
C(32)	40 (10)	1573 (3)	−3940 (9)	28 (3)
C(33)	−193 (11)	2003 (3)	−4180 (10)	26 (3)
C(34)	421 (10)	2289 (3)	−3290 (9)	26 (3)
C(35)	1236 (10)	2156 (3)	−2212 (9)	21 (3)
N(4)	2661 (9)	2224 (2)	−190 (8)	17 (2)
C(41)	1945 (10)	2432 (3)	−1197 (9)	18 (3)
C(42)	1911 (10)	2877 (3)	−1177 (9)	23 (3)
C(43)	2677 (11)	3081 (3)	−169 (10)	26 (3)
C(44)	3406 (10)	2865 (3)	844 (9)	19 (3)
C(45)	3379 (11)	2427 (3)	793 (9)	23 (3)
N(5)	3857 (8)	1715 (3)	1533 (7)	19 (2)
C(51)	4079 (10)	2131 (3)	1798 (9)	19 (3)
C(52)	4901 (10)	2267 (3)	2913 (8)	19 (3)
C(53)	5519 (11)	1972 (3)	3734 (10)	27 (3)
C(54)	5295 (11)	1546 (4)	3501 (9)	31 (3)
C(55)	4467 (10)	1429 (3)	2386 (9)	25 (3)
N(6)	5003 (14)	−284 (5)	7398 (13)	99 (5)
C(61)	4559 (15)	51 (5)	7303 (13)	66 (4)
C(62)	3986 (14)	465 (4)	7175 (12)	63 (4)
N(7)	10303 (12)	318 (3)	6927 (10)	62 (3)
C(71)	9452 (15)	362 (4)	6091 (13)	61 (4)
C(72)	8255 (14)	424 (5)	5023 (12)	78 (5)
N(8)	1770 (13)	779 (4)	4713 (12)	89 (4)
C(81)	1688 (14)	682 (4)	3714 (14)	65 (4)
C(82)	1554 (14)	571 (4)	2478 (11)	58 (4)

[a] Equivalent isotropic U defined as one-third of the trace of the orthogonalized U_{ij} tensor.

to some extent, $[Ni(terpy)Cl_2]$ has been used as the starting material in the present work. The chelating terpy ligand is expected to remain bonded to nickel during chloride substitution and to provide three N donor centers around the metal in the final products. Indeed, addition of 2 equiv of appropriate thiolates to $[Ni(terpy)Cl_2]$ in methanol or acetonitrile results in clean substitution of the chloride ligands with thiolates (eq 1). However,

$$[Ni(terpy)Cl_2] + 2RS^- \xrightarrow[\text{or } CH_3CN]{MeOH} \text{I, II, or III} \qquad (1)$$

with simple thiolates like PhS^-, only dimeric products like **1** (type I) are isolated. The propensity of thiolato sulfur to form bridges between metal centers as well as the additional stability acquired by Ni(II) (d^8 system) in octahedral coordination geometry favors dimer formation in these attempts. Since **1** has been crystallized

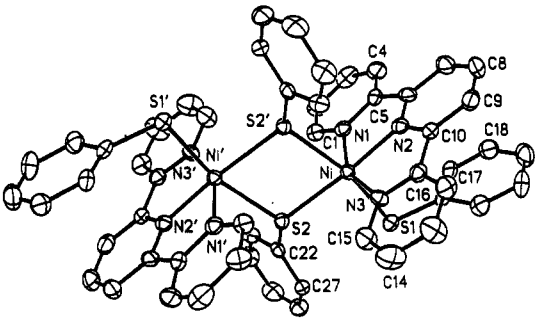

Figure 1. Computer-generated thermal ellipsoid (probability level 50%) plot of **1** with the atom-labeling scheme. Hydrogen atoms and solvent molecules of crystallization are omitted for clarity.

from dilute methanolic solution, it appears that the dimer is the predominant species in solution though spectral studies in donor solvents like DMSO (vide infra) indicate that monomeric species of the type II are formed under certain conditions. Bridge formation by thiolato sulfur in principle can be avoided by the use of less basic thiolates.[18] With this in mind, the weakly basic thiolate $C_6F_5S^-$ was used in our next attempt and as expected, reaction 1 affords complex **2** as the sole product when R = C_6F_5. In **2**, the two thiolate ligands do not form bridges between neighboring nickel centers. The metal ion is, however, six-coordinated with one solvent (CH_3CN) molecule occupying the sixth site (type II). Though complex **2** is a very good candidate for use in our eventual goal of studying reactions at the sixth site of nickel, it does not fulfill the need for genuine pentacoordinated Ni(II) complex(es) with the N_3S_2 chromophore in physical measurements like EXAFS. In our final attempt, the tendency of Ni(II) to achieve six-coordination has therefore been restricted by the use of bulky thiolates and the desired pentacoordinated product **3**[19] has been successfully isolated with 2,4,6-(i-Pr)$_3$C$_6$H$_2$S$^-$. The steric hindrance from the two bulky thiolate ligands is sufficient enough to keep the nickel center pentacoordinated though small molecules like CO can bind to the metal center under certain conditions (vide infra). The same thiolate has been used by other groups to synthesize various metal complexes of unusual coordination number and geometry.[20]

Structure of [Ni(terpy)(SPh)$_2$]$_2$·6CH$_3$OH (1). The molecular structure consists of centrosymmetric dimers of the composition [Ni(terpy)(SPh)$_2$]$_2$. A computer-generated drawing of the dimeric unit is shown in Figure 1 and selected bond distances and angles are collected in Table V. The coordination geometry around nickel is distorted octahedral with the three nitrogens of the terpy ligand occupying three coordination sites in the equatorial plane. The fourth equatorial site as well as one axial site is filled by the two thiolato sulfur atoms while the sixth axial site of each nickel is connected to the bridging equatorial thiolato sulfur from the other half of the dimer. The nonbridging thiolato sulfur is hydrogen bonded to one of the methanol molecules (S(1)···HO(2) = 2.59 (5) Å). A second methanol molecule is hydrogen-bonded to the first (O(2)···O(1) = 2.75 (5) Å). The Ni–Ni′ distance (3.920 (1) Å) is considerably longer compared to the same in simple homoleptic [Ni$_2$(SR)$_6$]$^{2-}$ complexes (e.g., 3.355 (2) Å with SR = SEt[21]). The S(2)–S(2)′ distance (2.991 Å) in **1** is however typical of the thiolato-bridged dimeric nickel(II) complexes.

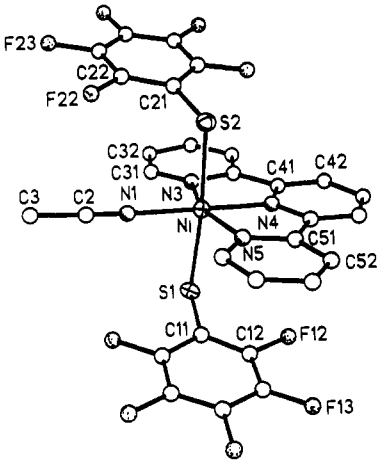

Figure 2. Computer-generated drawing of **2** with the atom-labeling scheme. Atoms that have been refined anisotropically are represented by thermal ellipsoids (probability level 50%). Hydrogen atoms and solvent molecules of crystallization are omitted for clarity.

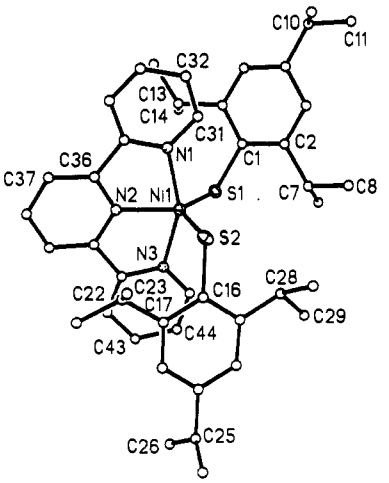

Figure 3. Computer-generated drawing of molecule A of **3** with the atom-labeling scheme. Anisotropically refined atoms are shown as thermal ellipsoids (probability level 50%). Hydrogen atoms and the solvent molecules of crystallization are omitted for clarity.

In tetrahedral[9] or square-planar[19] complexes, the Ni(II)–S distances lie in the range 2.1–2.3 Å. The same bond in Ni(II) complexes of higher coordination number is however significantly longer. For example, in *cis*-[Ni(bpy)$_2$(SPh)$_2$]·2D$_2$O,[7] the Ni(II)–S bonds are 2.444 (2) Å long. Likewise, long Ni(II)–S distances are observed in **1**, which also contains six-coordinated nickel centers. The nonbridging Ni(II)–S distance in **1** is 2.428 (2) Å while the bridging region comprises of one short (2.410 (2) Å) and one long (2.519 (2) Å) Ni(II)–S bonds (Table V). The Ni(II)–N bond lengths lie in the narrow range of 1.997 (5)–2.108 (4) Å and closely compare with those reported for terpy complexes of Ni(II).[22] Distortions from idealized octahedral geometry, caused by the "bite" of the terpy ligand are noticed in the N–Ni–N angles of 155.0 (2), 77.4 (2), and 77.7 (2)°. The S(1)–Ni–S(2)′ angle of 165.0 (1)° results from the near-parallel alignment and steric repulsion of the phenyl and the terpy rings.

Structure of [Ni(terpy)(SC$_6$F$_5$)$_2$(CH$_3$CN)]·3CH$_3$CN (2). A computer-generated drawing of the complex is shown in Figure 2 and selected bond distances and angles are listed in Table V. Molecules of the complex are well-separated from the three molecules of acetonitrile in the structure. The coordination geometry around nickel is distorted octahedral. The terpy ligand

(18) Dance, I. G. *Polyhedron* **1986**, *5*, 1057.
(19) As this paper was approaching completion, mention of a compound of composition [Ni(terpy)(S-2,4,6-(i-Pr)$_3$C$_6$H$_2$)$_2$] appeared: Corwin, D. T., Jr.; Koch, S. A.; Millar, M. M. *Abstracts of Papers*, 200th National Meeting of the American Chemical Society Washington, DC, 1990; INOR 271.
(20) (a) Corwin, D. T., Jr.; Koch, S. A. *Inorg. Chem.* **1988**, *27*, 493. (b) Corwin, D. T., Jr.; Fikar, R.; Koch, S. A. *Inorg. Chem.* **1987**, *26*, 3079. (c) Corwin, D. T., Jr.; Gruff, E. S.; Koch, S. A. *J. Chem. Soc., Chem. Commun.* **1987**, 966. (d) O'Sullivan, T.; Millar, M. M. *J. Am. Chem. Soc.* **1985**, *107*, 4096. (e) Fikar, R.; Koch, S. A.; Millar, M. M. *Inorg. Chem.* **1985**, *24*, 3311.
(21) Watson, A. D.; Rao, Ch. P.; Dorfman, J. R.; Holm, R. H. *Inorg. Chem.* **1985**, *24*, 2820.
(22) (a) Cortes, R.; Arriortua, M. I.; Rojo, T.; Solans, X.; Miravitlles, C.; Beltran, D. *Acta Crystallogr. Sect. C: Cryst. Struct. Commun.* **1985**, *C41*, 1733. (b) Arriortua, M. I.; Rojo, T.; Amigo, J. M.; Germain, G.; Declerq, J. P. *Bull. Soc. Chim. Belg.* **1982**, *91*, 337.

Table IV. Atomic Coordinates ($\times 10^4$) and Equivalent Isotropic Displacement Coefficients ($Å^2 \times 10^3$) for [Ni(terpy)(STripp)$_2$]·1.5CH$_3$CN (3)

	x	y	z	U(eq)[a]		x	y	z	U(eq)[a]
Ni(1)	381 (1)	3527 (1)	1805 (1)	14 (1)	N(5)	-5162 (4)	9862 (4)	3531 (4)	15 (2)
S(1)	-256 (1)	4657 (1)	2343 (1)	17 (1)	N(6)	-4345 (4)	10408 (4)	1947 (4)	16 (2)
S(2)	1610 (1)	2463 (1)	1937 (1)	19 (1)	C(46)	-2568 (5)	11139 (5)	1672 (5)	16 (2)
N(1)	-473 (4)	2641 (4)	2609 (4)	18 (2)	C(47)	-2972 (5)	11960 (5)	1322 (5)	18 (2)
N(2)	47 (4)	3284 (4)	1021 (4)	11 (1)	C(48)	-2626 (5)	12309 (5)	466 (5)	17 (2)
N(3)	1043 (4)	4332 (4)	677 (4)	13 (1)	C(49)	-1911 (5)	11887 (5)	-58 (5)	17 (2)
C(1)	-847 (5)	4276 (5)	3425 (5)	16 (2)	C(50)	-1532 (5)	11089 (5)	305 (5)	19 (2)
C(2)	-416 (5)	4073 (5)	3999 (5)	18 (2)	C(51)	-1828 (5)	10692 (5)	1151 (5)	14 (2)
C(3)	-875 (5)	3747 (5)	4840 (5)	17 (2)	C(52)	-3775 (5)	12457 (5)	1868 (5)	18 (2)
C(4)	-1743 (5)	3594 (5)	5136 (5)	20 (2)	C(53)	-4382 (6)	13099 (6)	1421 (6)	36 (2)
C(5)	-2155 (5)	3817 (5)	4562 (5)	17 (2)	C(54)	-3477 (6)	12866 (6)	2293 (5)	28 (2)
C(6)	-1737 (5)	4154 (5)	3723 (5)	18 (2)	C(55)	-1544 (6)	12226 (5)	-998 (5)	20 (2)
C(7)	530 (6)	4246 (5)	3703 (5)	23 (2)	C(56)	-1840 (6)	11798 (6)	-1403 (5)	31 (2)
C(8)	1050 (6)	3727 (6)	4272 (6)	40 (3)	C(57)	-1781 (6)	13198 (6)	-1310 (6)	33 (2)
C(9)	506 (6)	5190 (6)	3516 (6)	37 (3)	C(58)	-1393 (6)	9788 (5)	1482 (5)	24 (2)
C(10)	-2216 (6)	3185 (5)	6047 (5)	24 (2)	C(59)	-1099 (6)	9247 (6)	901 (6)	33 (2)
C(11)	-2161 (6)	3568 (6)	6637 (5)	32 (2)	C(60)	-631 (6)	9780 (6)	1724 (6)	35 (2)
C(12)	-1862 (6)	2226 (6)	6251 (6)	39 (3)	C(61)	-3443 (5)	7656 (5)	3394 (5)	16 (2)
C(13)	-2237 (5)	4382 (5)	3133 (5)	17 (2)	C(62)	-2662 (5)	7254 (5)	3617 (5)	16 (2)
C(14)	-2644 (6)	5333 (5)	2947 (5)	30 (2)	C(63)	-2737 (6)	6577 (5)	4321 (5)	21 (2)
C(15)	-2968 (6)	3868 (6)	3429 (6)	33 (2)	C(64)	-3522 (5)	6266 (5)	4806 (5)	17 (2)
C(16)	2553 (5)	2839 (5)	1079 (5)	16 (2)	C(65)	-4257 (5)	6638 (5)	4575 (5)	19 (2)
C(17)	2819 (5)	2672 (5)	310 (5)	19 (2)	C(66)	-4233 (5)	7323 (5)	3869 (5)	19 (2)
C(18)	3528 (6)	3011 (5)	-357 (5)	26 (2)	C(67)	-1766 (5)	7532 (5)	3080 (5)	16 (2)
C(19)	4000 (6)	3496 (6)	-300 (6)	30 (2)	C(68)	-1266 (6)	7083 (5)	2395 (5)	26 (2)
C(20)	3756 (6)	3646 (5)	454 (5)	24 (2)	C(69)	-1168 (6)	7398 (5)	3566 (5)	26 (2)
C(21)	3036 (6)	3340 (5)	1152 (5)	21 (2)	C(70)	-3557 (6)	5540 (5)	5602 (5)	22 (2)
C(22)	2331 (6)	2131 (5)	212 (5)	21 (2)	C(71)	-4245 (6)	4991 (6)	5877 (5)	30 (2)
C(23)	2671 (6)	1189 (6)	558 (6)	36 (2)	C(72)	-3729 (6)	5892 (6)	6307 (6)	34 (2)
C(24)	2385 (6)	2311 (6)	-680 (6)	39 (3)	C(73)	-5041 (5)	7667 (6)	3593 (5)	24 (2)
C(25)	4786 (7)	3850 (7)	-1047 (7)	49 (3)	C(74)	-4922 (6)	7211 (6)	2983 (5)	30 (2)
C(26)	4487 (9)	4566 (8)	-1646 (8)	79 (4)	C(75)	-5933 (6)	7565 (6)	4313 (5)	32 (2)
C(27A)	5616 (13)	3290 (13)	-1227 (12)	37 (5)	C(76)	-3246 (6)	8837 (5)	4427 (5)	24 (2)
C(27B)	5599 (18)	3733 (17)	-949 (16)	70 (8)	C(77)	-3364 (6)	8376 (6)	5262 (5)	30 (2)
C(28)	2737 (6)	3555 (6)	1968 (5)	29 (2)	C(78)	-4208 (6)	8299 (5)	5808 (5)	26 (2)
C(29)	3013 (7)	4368 (6)	1854 (6)	41 (3)	C(79)	-4943 (6)	8666 (5)	5558 (5)	24 (2)
C(30)	3102 (6)	2811 (6)	2591 (5)	30 (2)	C(80)	-4780 (5)	9101 (5)	4721 (5)	17 (2)
C(31)	-693 (6)	2318 (5)	3435 (5)	26 (2)	C(81)	-5479 (5)	9512 (5)	4347 (5)	18 (2)
C(32)	-1186 (6)	1671 (6)	3877 (6)	28 (2)	C(82)	-6387 (6)	9523 (6)	4781 (6)	30 (2)
C(33)	-1483 (6)	1365 (5)	3467 (5)	25 (2)	C(83)	-6952 (7)	9892 (6)	4339 (6)	34 (2)
C(34)	-1283 (5)	1706 (5)	2631 (5)	19 (2)	C(84)	-6636 (6)	10271 (5)	3499 (5)	26 (2)
C(35)	-768 (5)	2328 (5)	2214 (5)	16 (2)	C(85)	-5730 (5)	10248 (5)	3117 (5)	18 (2)
C(36)	-455 (5)	2696 (5)	1293 (5)	15 (2)	C(86)	-5259 (5)	10596 (5)	2215 (5)	14 (2)
C(37)	-650 (6)	2469 (5)	749 (5)	22 (2)	C(87)	-5705 (6)	11087 (5)	1658 (5)	24 (2)
C(38)	-306 (5)	2861 (5)	-84 (5)	23 (2)	C(88)	-5214 (6)	11355 (6)	825 (5)	27 (2)
C(39)	214 (5)	3476 (5)	-375 (5)	17 (2)	C(89)	-4299 (6)	11134 (5)	567 (5)	24 (2)
C(40)	386 (5)	3676 (5)	201 (5)	12 (2)	C(90)	-3880 (5)	10673 (5)	1138 (5)	16 (2)
C(41)	953 (5)	4279 (5)	0 (5)	11 (2)	N(7)	8827 (6)	157 (6)	5943 (6)	62 (3)
C(42)	1372 (5)	4752 (5)	-792 (5)	17 (2)	C(91)	9001 (7)	-174 (7)	7330 (6)	48 (3)
C(43)	1898 (5)	5293 (5)	-906 (5)	22 (2)	C(92)	8905 (7)	12 (6)	6554 (7)	41 (3)
C(44)	1996 (5)	5343 (5)	-215 (5)	19 (2)	N(8)	1144 (7)	799 (7)	5879 (7)	75 (3)
C(45)	1547 (5)	4864 (5)	553 (5)	16 (2)	C(93)	479 (8)	1525 (7)	4706 (8)	64 (4)
Ni(2)	-3856 (1)	9745 (1)	2938 (1)	14 (1)	C(94)	883 (8)	1128 (8)	5347 (8)	57 (3)
S(3)	-2991 (1)	10649 (1)	2765 (1)	18 (1)	N(9)	6721 (8)	779 (7)	8013 (7)	88 (4)
S(4)	-3399 (1)	8536 (1)	2508 (1)	15 (1)	C(95)	5003 (6)	1000 (6)	8702 (6)	35 (2)
N(4)	-3941 (4)	9180 (4)	4164 (4)	17 (2)	C(96)	5954 (8)	886 (7)	8331 (7)	48 (3)

[a] Equivalent isotropic U defined as one-third of the trace of the orthogonalized U_{ij} tensor. C(27A) and C(27B) are at 0.5 occupancy.

and the coordinated acetonitrile provide the four nitrogens in the equatorial plane while the two thiolates are trans to each other. The latter fact is presumably responsible for even longer Ni(II)–S bonds (2.482 (4) and 2.499 (4) Å). As viewed down the *b* axis, there is a noncrystallographic 2-fold axis passing through N(1), Ni, and N(4) (Figure S1, supplementary material). The planes of terpy and the C_6F_5 rings are nearly parallel with angles from the normal of 1.2 and 13.1° with respect to the terpy plane for rings bonded to S(1) and S(2), respectively. Metric parameters of the Ni(terpy) moiety in **2** are very similar to those observed with **1** (Table V).

Structure of [Ni(terpy)(S-2,4,6-(*i*-Pr)$_3$C$_6$H$_2$)$_2$]·1.5CH$_3$CN (3). The asymmetric unit contains two similar and well-separated molecules of the nickel complex and three isolated molecules of acetonitrile. Computer-generated drawings of the two molecules are shown in Figures 3 and 4. A diagram showing how the two molecules fit to each other is included in the supplementary material (Figure S2). The two molecules are very similar, the major differences arising from a 2.5° difference in the angles at the thiolate sulfurs and the rotational disposition of three of the six isopropyl groups. Of the atoms in the coordination sphere NiN_3S_2, there is a weighted RMS deviation of only 0.041 Å between the two molecules. Selected bond distances and angles are included in Table V.

In **3**, the coordination geometry at nickel is distorted trigonal bipyramidal (TBP). As one might expect, the two bulky thiolate ligands are coordinated in the equatorial plane. The central nitrogen of the terpy ligand is the third donor atom in this plane. The other two nitrogens of the terpy ligand occupy the two axial positions. Stabilization of the pentacoordinated structure is provided by the bulk of the two thiolate ligands. While the methyl groups of the isopropyl substituents bend away from the nickel center, the tertiary hydrogens are required to point toward it. A few short contacts between these tertiary hydrogens and nickel

Table V. Selected Bond Distances (Å) and Angles (deg) for Compounds **1–3**[a]

[Ni(terpy)(SPh)$_2$]$_2$·6CH$_3$OH (**1**)

Ni–S(1)	2.428 (2)	Ni–S(2)	2.410 (2)	S(2)–Ni(A)	2.519 (2)	N(1)–C(1)	1.329 (8)
Ni–N(1)	2.108 (4)	Ni–N(2)	1.997 (5)	N(1)–C(5)	1.348 (8)	N(2)–C(6)	1.348 (7)
Ni–N(3)	2.090 (5)	Ni–S(2A)	2.519 (2)	N(2)–C(10)	1.343 (8)	N(3)–C(11)	1.353 (8)
S(1)–C(16)	1.748 (5)	S(2)–C(22)	1.770 (6)	N(3)–C(15)	1.333 (8)	O(1)–C(28)	1.415 (8)
S(1)–Ni–S(2)	91.2 (1)	S(1)–Ni–N(1)	89.4 (1)	S(1)–Ni–S(2A)	165.0 (1)	S(2)–Ni–S(2A)	74.7 (1)
S(2)–Ni–N(1)	106.2 (1)	S(1)–Ni–N(2)	96.8 (1)	N(1)–Ni–S(2A)	89.7 (1)	N(2)–Ni–S(2A)	97.7 (1)
S(2)–Ni–N(2)	171.3 (1)	N(1)–Ni–N(2)	77.4 (2)	N(3)–Ni–S(2A)	95.5 (1)	Ni–S(1)–C(16)	105.3 (2)
S(1)–Ni–N(3)	91.7 (1)	S(2)–Ni–N(3)	98.7 (1)	Ni–S(2)–C(22)	155.2 (2)	Ni–S(2)–Ni(A)	105.3 (1)
N(1)–Ni–N(3)	155.0 (2)	N(2)–Ni–N(3)	77.7 (2)	C(22)–S(2)–Ni(A)	125.3 (2)	Ni–N(1)–C(1)	127.0 (4)

[Ni(terpy)(C$_6$F$_5$S)$_2$(CH$_3$CN)]·3CH$_3$CN (**2**)

Ni–S(1)	2.482 (4)	Ni–S(2)	2.499 (4)	N(1)–C(2)	1.114 (13)	C(2)–C(3)	1.456 (15)
Ni–N(1)	2.047 (8)	Ni–N(3)	2.085 (7)	N(3)–C(31)	1.315 (12)	N(3)–C(35)	1.391 (13)
Ni–N(4)	1.987 (7)	Ni–N(5)	2.080 (7)	N(4)–C(41)	1.356 (12)	N(4)–C(45)	1.330 (12)
S(1)–C(11)	1.745 (9)	C(12)–F(12)	1.360 (11)	N(5)–C(51)	1.359 (13)	N(5)–C(55)	1.353 (12)
S(2)–C(21)	1.755 (9)	C(22)–F(22)	1.361 (12)	N(6)–C(61)	1.147 (21)	N(7)–C(71)	1.113 (16)
S(1)–Ni–S(2)	175.0 (1)	S(1)–Ni–N(1)	87.9 (3)	N(4)–Ni–N(5)	78.9 (3)	Ni–S(1)–C(11)	102.8 (4)
S(2)–Ni–N(1)	87.1 (3)	S(1)–Ni–N(3)	86.0 (3)	S(1)–C(11)–C(12)	123.6 (8)	S(1)–C(11)–C(16)	123.5 (7)
S(2)–Ni–N(3)	94.4 (3)	N(1)–Ni–N(3)	100.7 (3)	Ni–S(2)–C(21)	102.8 (4)	S(2)–C(21)–C(22)	122.9 (7)
S(1)–Ni–N(4)	93.1 (3)	S(2)–Ni–N(4)	91.8 (3)	Ni–N(1)–C(2)	178.2 (11)	N(1)–C(2)–C(3)	179.3 (11)
N(1)–Ni–N(4)	178.9 (4)	N(3)–Ni–N(4)	79.3 (3)	Ni–N(3)–C(31)	127.9 (7)	Ni–N(3)–C(35)	114.2 (6)
S(1)–Ni–N(5)	94.9 (3)	S(2)–Ni–N(5)	86.6 (3)	Ni–N(4)–C(41)	118.2 (6)	Ni–N(4)–C(45)	119.7 (6)
N(1)–Ni–N(5)	101.2 (3)	N(3)–Ni–N(5)	158.1 (3)	Ni–N(5)–C(51)	114.1 (6)	Ni–N(5)–C(55)	127.7 (6)

[Ni(terpy)(S-2,4,6-(*i*-Pr)$_3$C$_6$H$_2$)$_2$]·1.5CH$_3$CN (**3**)

Ni(1)–S(1)	2.274 (3)	Ni(1)–S(2)	2.332 (2)	Ni(2)–S(3)	2.298 (3)	Ni(2)–S(4)	2.302 (3)
Ni(1)–N(1)	2.113 (7)	Ni(1)–N(2)	1.974 (9)	Ni(2)–N(4)	2.075 (7)	Ni(2)–N(5)	1.968 (6)
Ni(1)–N(3)	2.086 (5)	S(1)–C(1)	1.779 (7)	Ni(2)–N(6)	2.125 (7)	S(3)–C(46)	1.789 (7)
S(2)–C(16)	1.779 (7)	N(1)–C(31)	1.344 (11)	S(4)–C(61)	1.771 (7)	N(4)–C(76)	1.340 (13)
N(1)–C(35)	1.355 (15)	N(2)–C(36)	1.335 (12)	N(4)–C(80)	1.354 (9)	N(5)–C(81)	1.330 (9)
N(2)–C(40)	1.352 (9)	N(3)–C(41)	1.363 (13)	N(5)–C(85)	1.342 (12)	N(6)–C(86)	1.366 (10)
N(3)–C(45)	1.331 (13)	C(1)–C(2)	1.416 (15)	N(6)–C(90)	1.333 (9)	C(46)–C(47)	1.412 (10)
S(1)–Ni(1)–S(2)	130.1 (1)	S(1)–Ni(1)–N(1)	103.4 (2)	S(3)–Ni(2)–S(4)	128.2 (1)	S(3)–Ni(2)–N(4)	91.3 (2)
S(2)–Ni(1)–N(1)	89.1 (2)	S(1)–Ni(1)–N(2)	126.0 (2)	S(4)–Ni(2)–N(4)	98.3 (2)	S(3)–Ni(2)–N(5)	125.0 (2)
S(2)–Ni(1)–N(2)	103.7 (2)	N(1)–Ni(1)–N(2)	78.1 (3)	S(4)–Ni(2)–N(5)	106.7 (2)	N(4)–Ni(2)–N(5)	78.2 (3)
S(1)–Ni(1)–N(3)	88.9 (2)	S(2)–Ni(1)–N(3)	98.4 (2)	S(3)–Ni(2)–N(6)	100.9 (2)	S(4)–Ni(2)–N(6)	89.9 (2)
N(1)–Ni(1)–N(3)	156.3 (4)	N(2)–Ni(1)–N(3)	78.3 (3)	N(4)–Ni(2)–N(6)	156.5 (2)	N(5)–Ni(2)–N(6)	78.3 (3)
Ni(1)–S(1)–C(1)	108.1 (3)	Ni(1)–S(2)–C(16)	105.2 (3)	Ni(2)–S(3)–C(46)	105.5 (4)	Ni(2)–S(4)–C(61)	107.7 (3)
Ni(1)–N(1)–C(31)	127.7 (8)	Ni(1)–N(1)–C(35)	114.1 (5)	Ni(2)–N(4)–C(76)	125.8 (5)	Ni(2)–N(4)–C(80)	115.0 (6)
C(31)–N(1)–C(35)	118.0 (8)	Ni(1)–N(2)–C(36)	120.1 (5)	C(76)–N(4)–C(80)	118.9 (7)	Ni(2)–N(5)–C(81)	119.2 (6)
Ni(1)–N(2)–C(40)	119.0 (7)	C(36)–N(2)–C(40)	120.7 (9)	Ni(2)–N(5)–C(85)	120.9 (5)	C(81)–N(5)–C(85)	119.9 (7)
Ni(1)–N(3)–C(41)	114.9 (6)	Ni(1)–N(3)–C(45)	127.3 (6)	Ni(2)–N(6)–C(86)	112.6 (5)	Ni(2)–N(6)–C(90)	128.7 (6)

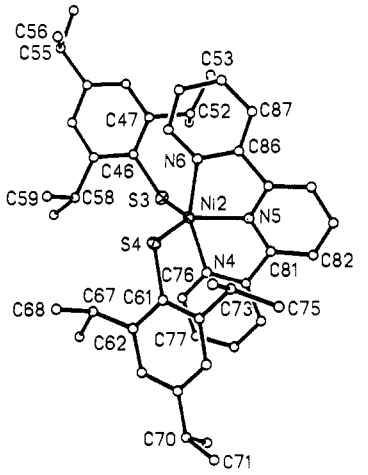

Figure 4. Computer-generated drawing of molecule B of **3** with the atom-labeling scheme. Anisotropically refined atoms are shown as thermal ellipsoids (probability level 50%). Hydrogen atoms and the solvent molecules of crystallization are omitted for clarity.

prevent the metal center from further coordination. In the structure shown in Figure 3, examples of such contacts are Ni(1)···H(7) = 3.51 Å and Ni(1)···H(13) = 3.34 Å while in the other molecule (Figure 4) Ni(2)···H(58) = 3.05 Å and Ni(2)···H(73) = 3.44 Å.

The Ni(II)–S distances in **3** (2.274 (3)–2.332 (2) Å) are noticeably shorter than those observed with **1** and **2** (Table V). This fact clearly demonstrates the variability of the Ni(II)–S distance with coordination number. Dimensions of the Ni(terpy) portion of **3** are however very similar to those already noted for **1** and **2**. The S–Ni–S angle (129° average value) deviates from the ideal value of 120° due to steric requirement.

Properties. In the solid state, the complexes **1–3** are moderately air stable, **1** being the most sensitive to oxygen. Solutions in methanol or acetonitrile, however, decompose on exposure to air. In general, solution stability is enhanced when DMSO is used as the solvent. The complexes **1–3** respectively give rise to deep reddish brown, orange, and purple solutions in this solvent which has been used in most spectroscopic measurements (Table VI). The electronic absorption spectra of all three complexes exhibit several bands of very different intensities (Table VI). At the present time, no attempt has been made to assign these complicated spectra.[23] The electronic absorption spectrum of **1** in DMSO is distinctly different from that in methanol or acetonitrile. However, the general appearance of the absorption spectrum of each of these complexes in DMSO is quite similar. It thus appears that in DMSO, **1** exists as the solvated monomer [Ni(terpy)(SPh)$_2$(solv)] (i.e., a type II species). This conclusion is also supported by the NMR spectra of **1–3**. Since crystallization from methanol or acetonitrile always affords the dimer **1**, we believe that in these solvents the solvated monomer $\rightleftarrows$ S-bridged dimer equilibrium lies almost exclusively to the right.

(23) Distorted coordination geometries, asymmetric crystal fields and presence of both d–d and charge-transfer transitions all make the task of assignment a difficult one: Lever, A. B. P. In *Inorganic Electronic Spectroscopy*, 2nd ed.; Elsevier: Amsterdam, 1984; pp 507–530.

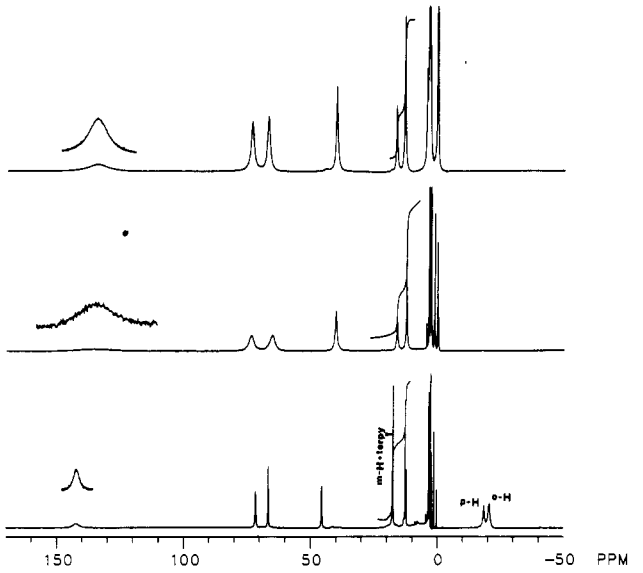

Figure 5. ^{1}H NMR spectra (300 MHz) of [Ni(terpy)Cl$_2$] (top trace), **2** (middle trace), and **1** (bottom trace) in $(CD_3)_2SO$. Signal assignments for the protons of the thiolate ligands in **1** are indicated. The signal from the meta Hs overlap with one of the terpy resonances in the ~20 ppm region.

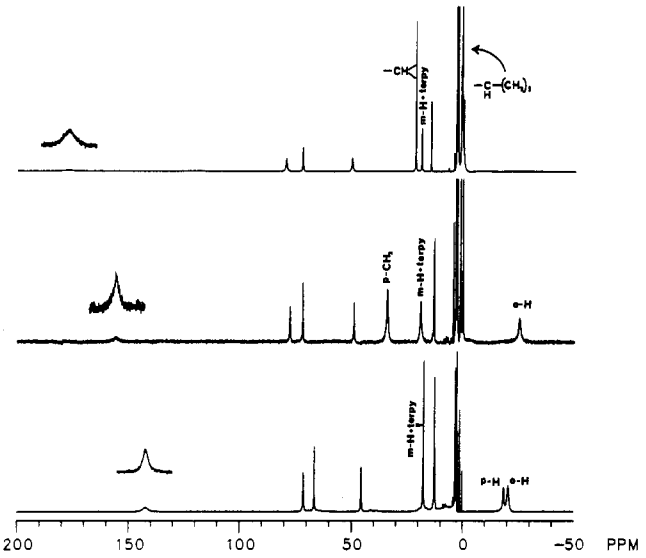

Figure 6. ^{1}H NMR spectra (300 MHz) of **3** (top trace), [Ni(terpy)(S-C_6H_4-*p*-CH_3)$_2$]$_2$ (middle trace), and **1** (bottom trace) in $(CD_3)_2SO$. Signal assignments for the protons of the thiolate ligands are indicated. In all three cases, the meta H signal overlaps with one of the terpy signals in the ~20 ppm region.

The ^{1}H NMR spectra of the complexes have been recorded in $(CD_3)_2SO$ (Table VI; Figures 5 and 6). Several paramagnetically shifted resonances are observed. Comparison of the ^{1}H NMR spectra of **1**, **2**, and [Ni(terpy)Cl$_2$] (Figure 5) clearly identifies the three (ortho, meta and para Hs) resonances of the PhS$^-$ ligand. In both Figure 5 and 6, the spectrum shown for **1** is the one recorded at 323 K. At 293 K (the temperature for all other spectra), the resonances due to ortho and para Hs are broad and overlap to some extent. That the peak corresponding to meta H coincides with one of the terpy peaks in the ~18 ppm region is evident from the integrated area under that signal (Figure 5). The para H resonance has been assigned by the use of the *p*-$CH_3C_6H_4S^-$ ligand. In the NMR spectrum of [Ni(terpy)-(SC_6H_4-*p*-CH_3)$_2$]$_2$ (Figure 6, middle trace), the *p*-CH_3 group gives rise to a peak at 34.05 ppm while on the high-field side of TMS, only one peak due to ortho H is recorded at −25.45 ppm. This in turn identifies the two signals at −18.75 and −20.76 ppm in the spectrum of **1** as the peaks corresponding to para and ortho H, respectively (intensity ratio 1:2). With **3**, peaks due to the methyl

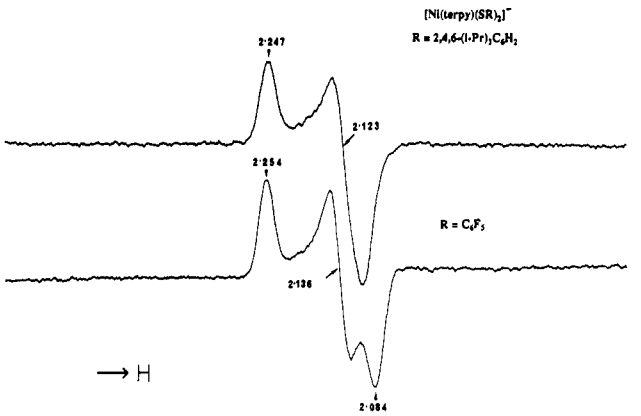

Figure 7. X-Band EPR spectra (100 K) of [Ni(terpy)(SR)$_2$]$^-$ (**4**) in DMF. Selected *g* values are indicated. Spectrometer settings: microwave frequency, 9.43 GHz; microwave power, 13 mW; modulation frequency, 100 kHz; modulation amplitude, 2G.

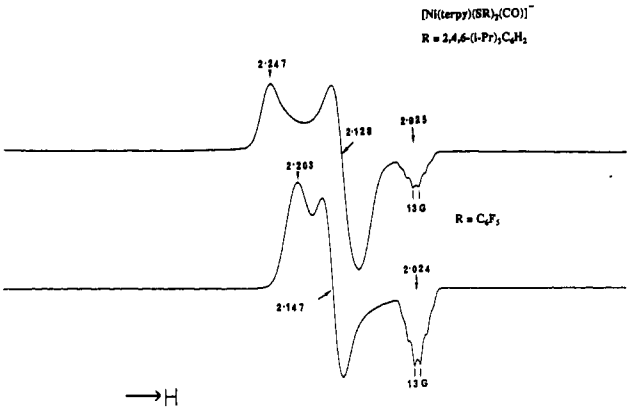

Figure 8. X-Band EPR spectra (100 K) of [Ni(terpy)(SR)$_2$(CO)]$^-$ (**5**) in DMF. Selected *g* and *A* values are indicated. Spectrometer settings are the same as in Figure 7.

groups and the tertiary H of the isopropyl unit are located at 0.73 and 21.55 ppm, respectively, while the meta Hs resonate at 18.87 ppm along with one terpy signal. With each complex, six separate peaks due to six sets of terpy hydrogen(s) have been recorded (Table VI). Peaks noted in the 0–5 ppm correspond to the residual protons in $(CD_3)_2SO$, the solvent molecules of crystallization, and TMS. A general pattern emerges out of the six spectra shown in Figures 5 and 6, which again suggests that **1** is most probably present as [Ni(terpy)(SPh)$_2$(solv)] in DMSO solution. It is somewhat difficult to predict whether a molecule of DMSO is coordinated to the nickel center in **3** or not, though on steric grounds a pentacoordinated species is the preferred one.

Results of EPR studies on hydrogenase from *Chromatium vinosum* indicate that both H$^-$ and CO bind to nickel at the same ligand position.[24] Following establishment of type II and III structures, we have initiated studies on binding of H$^-$ and CO to the nickel centers of **2** and **3** in solvents like DMF.[25] Passage of CO through a solution of **2** or **3** in DMF as such does not bring about any change in color. Addition of $Na_2S_2O_4$ to these DMF solutions on the other hand results in rapid color changes to greenish brown or orange. Frozen samples of such solutions exhibit strong EPR signals. In the case of **2**, a rhombic signal with g_1 = 2.254, g_2 = 2.136, and g_3 = 2.084 (Figure 7, bottom trace) is recorded while with **3** an axial spectrum with $g_\parallel$ = 2.247 and $g_\perp$ = 2.123 (Figure 7, top trace) is observed. These spectra clearly

(24) (a) van der Zwaan, J. W.; Albracht, S. P. J.; Fontijn, R. D.; Roelofs, Y. B. M. *Biochim. Biophys. Acta* **1986**, *872*, 208. (b) van der Zwaan, J. W.; Albracht, S. P. J.; Fontijn, R. D.; Slater, E. C. *FEBS Lett.* **1985**, *179*, 271.

(25) Inspection of CPK model of **3** reveals a rather limited amount of space around nickel for further coordination. However, small ligands like H$^-$ or CO can reach the metal center without hindrance.

Table VI. Spectroscopic Data

Electronic Absorption spectral Data (Solvent DMSO)

complex	λ_{max}, nm (ϵ, M^{-1} cm^{-1})
1	1020 (103), 430 (7350), 310 (54000), 283 (54000)
2	1010 (45), 480 sh (400), 335 sh (22000), 320 (26000), 284 (55000)
3	990 (57), 510 (6400), 430 sh (3750), 312 sh (25000), 284 (33000)

^{1}H NMR Spectral Data (Solvent $(CD_3)_2SO$, δ (ppm) from TMS)[a,b]

complex	δ
$[Ni(terpy)Cl_2]$	135.19, 73.29, 66.79, 39.76, 15.86, 12.56 (2.50)
2	136.34, 73.44, 65.16, 40.16, 15.97, 12.27 (2.50, 2.08)
1	141.72, 71.28, 66.35, 45.43, 17.34,[c] 12.52 (4.11, 3.17, 2.50), *-18.75*, *-20.76*
$[Ni(terpy)(S\text{-}C_6H_4\text{-}p\text{-}CH_3)_2]_2$	156.12, 77.46, 71.85, 49.06, *34.05*, 18.92,[c] 13.09 (4.10, 3.17, 2.50), *-25.45*
3	177.30, 79.47, 72.09, 50.28, *21.55*, 18.87,[c] 14.66 (2.50, 2.08), *0.73*

EPR Spectral Data (DMF Glass, 100 K, g Values (A in G))[d]

complex	g
$[Ni(terpy)(SC_6F_5)_2]^-$	2.254, 2.136, 2.084
$[Ni(terpy)(S\text{-}2,4,6\text{-}(i\text{-}Pr)_3C_6H_2)_2]^-$	2.247, 2.123
$[Ni(terpy)(SC_6F_5)_2(CO)]^-$	2.203, 2.147, 2.024 (3)
$[Ni(terpy)(S\text{-}2,4,6\text{-}(i\text{-}Pr)_3(C_6H_2)_2(CO)]^-$	2.247, 2.128, 2.025 (13)
$[Ni(terpy)(S\text{-}2,4,6\text{-}(i\text{-}Pr)_3C_6H_2)_2(H)]^-$	2.238, 2.191, 2.045

[a] Peak positions for protons of the thiolate ligands are in italics and those for solvents are in parentheses. [b] All the spectra have been recorded at 293 K except for **1** in which case the probe temperature was 323 K (see text). At 293 K, the δ values for **1** are 154.92, 76.76, 71.81, 48.77, 17.87,[c] 13.26 (4.10, 3.17, 2.50), *-19.06*, and *-22.15* ppm. [c] The meta H peak of the thiolate overlaps with this terpy peak (see Figures 5 and 6). [d] Spectrometer settings: microwave frequency, 9.43 GHz; microwave power, 13 mW; modulation frequency, 100 kHz; modulation amplitude, 2 G.

indicate that the nickel centers in **2** and **3** are reduced by dithionite[26] (eq 2). The reduced species $[Ni(terpy)(SR)_2]^-$, R =

$$\mathbf{3} \xrightarrow[DMF]{Na_2S_2O_4} \underset{\mathbf{4}}{[Ni(terpy)(SR)_2]^-} \xrightarrow{CO} \underset{\mathbf{5}}{[Ni(terpy)(SR)_2(CO)]^-} \quad (2)$$

$$R = C_6F_5,\ 2,4,6\text{-}(i\text{-}Pr)_3C_6H_2$$

C_6F_5, 2,4,6-$(i$-$Pr)_3C_6H_2$ (**4**), are short-lived even at low temperatures. When the reduction is performed in DMF that has been saturated with CO, the resultant species give rise to rhombic EPR spectra (Figure 8; Table VI). The g_3 region, in both cases, exhibits at least six resolved lines with a hyperfine coupling constant (A) of 13 G. Though assignment of the EPR spectra of Ni(I) complexes with distorted coordination geometries is a rather difficult task,[27] it appears that the spectra displayed in Figure 8 arise from distorted octahedral nickel(I) complexes $[Ni(terpy)(SR)_2(CO)]^-$, R = C_6F_5, 2,4,6-$(i$-$Pr)_3C_6H_2$ (**5**) with the two bulky thiolate ligands trans to each other (eq 2). Such a structure contains three terpy nitrogens and the CO ligand in the equatorial plane. Since the unpaired electron of Ni(I) (d^9 system) usually resides in the $d_{x^2-y^2}$ orbital ($g_{zz} > g_{xx}, g_{yy}$),[28] hyperfine interaction with three nitrogens is expected to generate seven lines. The CO adducts **5** are more stable than **4**. The same EPR spectra were recorded

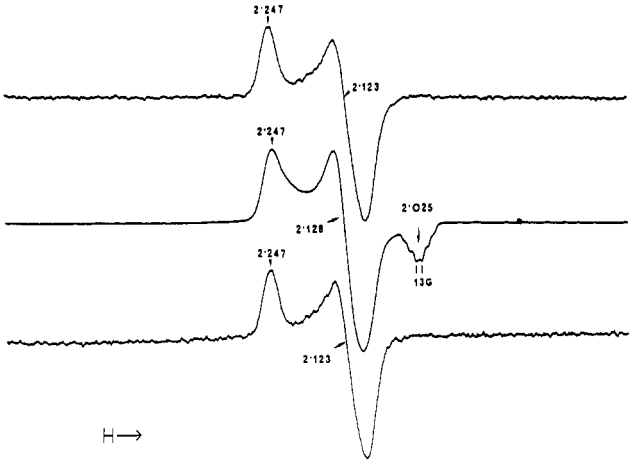

Figure 9. X-Band EPR spectra (100 K) of $[Ni(terpy)(S\text{-}2,4,6\text{-}(i\text{-}Pr)_3C_6H_2)_2]^-$ (top trace) and the CO adduct $[Ni(terpy)(S\text{-}2,4,6\text{-}(i\text{-}Pr)_3C_6H_2)_2(CO)]^-$ (middle trace) in DMF. The spectrum at the bottom was obtained with the same EPR sample of the CO adduct following passage of N_2 through the solution at −40 °C for 5 min. Selected g and A values are indicated. Spectrometer settings are the same as in Figure 7.

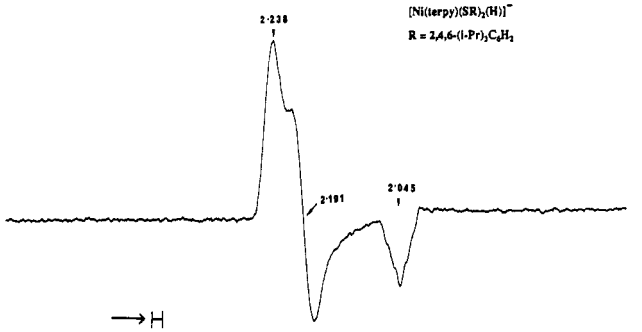

Figure 10. X-Band EPR spectrum (100 K) of $[Ni(terpy)(S\text{-}2,4,6\text{-}(i\text{-}Pr)_3C_6H_2)(H)]^-$ in DMF. Spectrometer settings are the same as in Figure 7.

after samples of **5** have been stored at −20 °C for 24 h.

An interesting consequence of steric crowding is noted in the CO-binding reaction (i.e., conversion of **4** to **5**) with R = 2,4,6-$(i$-$Pr)_3C_6H_2$. When dinitrogen is passed through the EPR sample of $[Ni(terpy)(S\text{-}2,4,6\text{-}(i\text{-}Pr)_3C_6H_2)_2(CO)]^-$ for 3–4 min at −40 °C and the solution refrozen, the spectrum reverts to that of $[Ni(terpy)(S\text{-}2,4,6\text{-}(i\text{-}Pr)_3C_6H_2)_2]^-$ (Figure 9). This result implies that CO binding at the nickel center of $[Ni(terpy)(S\text{-}2,4,6\text{-}(i\text{-}Pr)_3C_6H_2)_2]^-$ is reversible. In contrast, no change is observed when dinitrogen is passed through the EPR sample of $[Ni(terpy)(SC_6F_5)_2(CO)]^-$. Clearly, CO is more tightly bound to the nickel center in the latter complex, which is less crowded. The decreased basicity of the $C_6F_5S^-$ ligands could also be partially responsible for this difference.

Reaction of **3** with $NaBH_4$ in DMF at low temperature (−40 °C) affords a product that exhibits a rhombic EPR signal with $g_1 = 2.238$, $g_2 = 2.191$, and $g_3 = 2.045$ (Figure 10). The g_3 region of the spectrum consists of at least five resolved lines due to hyperfine coupling. Since this spectrum resembles the ones displayed in Figure 8, we propose that the spectrum arises from the hydride adduct of **3**, i.e., $[Ni(terpy)(S\text{-}2,4,6\text{-}(i\text{-}Pr)_3C_6H_2)_2(H)]^-$. This species is moderately stable at low temperature. We have as yet been unsuccessful in recording the EPR spectrum of the hydride adduct of **2**. Nevertheless, it is encouraging to note that both CO and H^- bind to the nickel center of **3**, a behavior exhibited by the nickel site of the enzyme. At the present time, attempts are being made to collect more spectral data on **4**, **5**, and the hydride adduct(s). Elaborate EXAFS, electrochemical, and EPR measurements at other frequencies are also in progress. The results will be reported elsewhere.

Acknowledgment. Financial support from the donors of the

(26) (a) Lapin, A. G.; McAuley, A. *Adv. Inorg. Chem.* **1988**, *32*, 241. (b) Nag, K.; Chakravorty, A. *Coord. Chem. Rev.* **1980**, *33*, 87.
(27) Salerno, J. C. In *The Bioinorganic Chemistry of Nickel*; Lancaster, J. R., Jr., Ed.; VCH Publishers: New York, 1988; Chapter 3.
(28) Moura, J. J. G.; Teixeira, M.; Moura, I.; LeGall, J. In *The Bioinorganic Chemistry of Nickel*; Lancaster, J. R., Jr., Ed.; VCH Publishers: New York, 1988; Chapter 9.

Petroleum Research Fund, administered by the American Chemical Society, is gratefully acknowledged.

Supplementary Material Available: View down the *b* axis showing the noncrystallographic 2-fold axis in **2** (Figure S1), diagram showing the fit of the two molecules of complex **3** present in the asymmetric unit (Figure S2), and crystal structure data for **1-3**, including complete lists of bond lengths (Tables S1-S3) and angles (Tables S4-S6), anisotropic thermal parameters (Tables S7-S9), and H-atom coordinates (Tables S10-S12) (14 pages); listings of observed and calculated structure factors (Tables S13-S15) (89 pages). Ordering information is given on any current masthead page.

Contribution from the Department of Inorganic Chemistry, The University of Sydney, Sydney, NSW 2006, Australia

Molecular Mechanics Analysis of the Stereochemical Factors Influencing Monofunctional and Bifunctional Binding of *cis*-Diamminedichloroplatinum(II) to Adenine and Guanine Nucleobases in the Sequences d(GpApGpG)·d(CpCpTpC) and d(GpGpApG)·d(CpTpCpC) of A- and B-DNA

Trevor W. Hambley

Received January 17, 1990

Monofunctional and bifunctional binding of *cis*-diamminedichloroplatinum(II) (DDP) to the guanine and/or adenine bases of the sequences d(GpApGpG)·d(CpCpTpC) and d(GpGpApG)·d(CpTpCpC) of A- and B-DNA have been modeled by molecular mechanics. The stereochemical factors that influence the tendencies for sequence specific binding are described. Monofunctional binding of DDP produces significant changes in the conformational geometry of the DNA. In particular, the bases are rotated by up to 20°, altering the distance from the Pt atom to potential binding sites on adjacent residues and making the distances to the 5'- and 3'-bases approximately equal. This is in contrast to the unequal distances predicted on the basis of idealized models of A- and B-DNA. Models for bifunctional adducts with ApG sequences are similar to those seen for bifunctional adducts with GpG sequences in that an NH_3 ligand makes a hydrogen bond with O6 of the 3'-guanine. In contrast, models for bifunctional adducts with GpA sequences have a highly unfavorable contact between the equivalent NH_3 ligand and the NH_2 of the 3'-adenine. Five-coordinate transition-state models show that these interactions persist and are potentially important in determining the frequency of occurrence of the A*pG* and G*pA* adducts.

Introduction

It is now generally accepted that the mechanism of action of the anticancer drug DDP (DDP = *cis*-diamminedichloroplatinum(II), *cis*-[$Pt(NH_3)_2Cl_2$]) involves binding to DNA.[1,2] In vitro studies of the interaction of DDP with DNA or fragments of DNA show that the bulk of DDP is bound to the N7 atoms of the nucleobases guanine and adenine.[3-5] The major binding site was found to be adjacent guanine bases of the one strand [d(G*pG*)] with a smaller amount bound to the d(A*pG*) sequence.[3,4] Binding to d(GpA) sequences was not found, or occurred at very low frequency, in binding studies with DNA[3,4] and the trinucleotide d(GpApG).[5] The lower preference for d(A*pG*) binding compared with d(G*pG*) binding is understandable on the basis of the lower kinetic preference for binding to adenine compared with guanine.[6,7] However, this does not explain why binding does not occur to d(GpA) sequences. Dewan has pointed out that when DDP binds to the central guanine in a d(ApGpA) sequence of B-DNA, the distance from the Pt atom to the N7 of the adenine on the 5'-side is ~3 Å and the distance to the N7 of the adenine on the 3'-side is ~5 Å.[8] This observation is consistent with some kinetic preference for the formation of d(A*pG*) adducts over d(G*pA*) adducts. However, we question whether such a difference is sufficient to account for the apparently complete absence of the latter adduct in some binding experiments,[3,4] especially when it is remembered that DDP has been found to bind appreciably to d(G*pNpG*) sequences,[5] in which the initial separation of the bases is likely to be 7-8 Å.

In a preliminary molecular mechanics study of the binding of DDP to the sequences d(CpApG)·d(CpTpC) and d(GpGpA)·d(TpCpC), we have shown that formation of d(G*pA*) adducts results in an unfavorable interaction, between an ammine group of DDP and the NH_2 group of the adenine base, not observed in the formation of the d(A*pG*) adduct.[9] While direct conclusions cannot be drawn from these models because binding of DDP, particularly to adenine nucleobases, is probably kinetically rather than thermodynamically controlled,[10] we propose that this type of destabilizing interaction would occur during the binding process and so strongly inhibit formation of the d(G*pA*) adduct. In order to investigate further this and other factors that might stereochemically influence binding of DDP to adenine-containing sequences, we have modeled the monofunctional and bifunctional binding of DDP to the sequences d(GpApGpG)·d(CpCpTpC) and d(GpGpApG)·d(CpTpCpC) (hereafter GAGG and GGAG) and report the results herein. Five-coordinate models for the transition state leading to the formation of the bifunctional models have also been studied. Mindful of recent studies which have shown that the structure of DNA is strongly sequence dependent[11] and that its solution structure is not limited to the B form[11c] we have considered models based on both A-DNA and B-DNA.

Experimental Section

The Model. Strain energies were calculated according to the formalism

$$E_{tot} = \sum E_b + \sum E_\theta + \sum E_\varphi + \sum E_\sigma + \sum E_{nb} + \sum E_{hb} + \sum E_\epsilon$$

where E_b represents bond deformation energy, E_θ valence angle defor-

(1) Roberts, J. J. *Adv. Inorg. Biochem.* **1981**, *3*, 274-332.
(2) Pinto, A. L.; Lippard, S. J. *Biochim. Biophys. Acta* **1985**, *780*, 167-180.
(3) Eastman, A. *Biochemistry* **1983**, *22*, 3927-3933.
(4) Fichtinger-Schepman, A. M. J.; van der Veer, J. L.; den Hartog, J. H. J.; Lohman, P. H. M.; Reedijk, J. *Biochemistry* **1985**, *24*, 707-713.
(5) van der veer, J. L.; van den Elst, H.; den Hartog, J. H. J.; Fichtinger-Schepman, A. M. J.; Reedijk, J. *Inorg. Chem.* **1986**, *25*, 4657-4663.
(6) Martin, R. B. *Acc. Chem. Res.* **1985**, *18*, 32-38.
(7) Kim, S.-H.; Martin, R. B. *Inorg. Chim. Acta* **1984**, *91*, 11-18.
(8) Dewan, J. C. *J. Am. Chem. Soc.* **1984**, *106*, 7239-7244.
(9) Hambley, T. W. *J. Chem. Soc., Chem. Commun.* **1988**, 221-223.
(10) Johnson, N. P.; Mazard, A. M.; Escalier, J.; Macquet, J. P. *J. Am. Chem. Soc.* **1985**, *107*, 6376-6380.
(11) (a) Dickerson, R. E.; Drew, H. R. *J. Mol. Biol.* **1981**, *149*, 761-786. (b) Lomononssoff, G. P.; Butler, P. J. G.; Klug, A. *J. Mol. Biol.* **1981**, *149*, 745-760. (c) Drew, H. R.; McCall, M. J.; Calladine, C. R. *Biol. Aspects DNA Topol.*, submitted for publication.

0020-1669/91/1330-0937$02.50/0